



# Direct electrosynthesis of methylamine from carbon dioxide and nitrate

Yueshen Wu<sup>1,2,4</sup>, Zhan Jiang<sup>3,4</sup>, Zhichao Lin<sup>3,4</sup>, Yongye Liang<sup>3</sup>✉ and Hailiang Wang<sup>1,2</sup>✉

**The electrochemical reduction of carbon dioxide is an appealing technology that stores renewable electricity in the chemical form and has the potential to transform the way carbon fuels are utilized today. While there have been successes in the electro-synthesis of alkanes, alkenes and alcohols, access to organonitrogen molecules such as alkylamines remains largely beyond the reach of current electrocatalysis. Here we report the first electrochemical reaction that converts carbon dioxide and nitrate to methylamine in aqueous media under ambient conditions catalysed by a cobalt  $\beta$ -tetraaminophthalocyanine molecular catalyst supported on carbon nanotubes. The overall reaction, involving the transfer of 14 electrons and 15 protons to form each methylamine molecule, is an eight-step catalytic cascade process enabled by the coupling of two reactive intermediates near the catalyst surface. The key C-N bond-forming step is found to be the spillover of hydroxylamine from nitrate reduction and its subsequent condensation with formaldehyde from carbon dioxide reduction. This study provides a successful example of sustainable alkylamine synthesis from inorganic carbon and nitrogen wastes, which could contribute to greenhouse gas mitigation for a carbon-neutral future.**

Electrochemical synthesis from cheap and abundant inorganic reactants such as carbon dioxide (CO<sub>2</sub>) and nitrate (NO<sub>3</sub><sup>-</sup>) is a promising approach to the sustainable production of valuable chemicals<sup>1–5</sup>. Existing examples include CO<sub>2</sub> reduction to alcohols<sup>6–9</sup> and NO<sub>3</sub><sup>-</sup> reduction to ammonia (NH<sub>3</sub>)<sup>10–13</sup>. Both CO<sub>2</sub> and NO<sub>3</sub><sup>-</sup> are chemical species of environmental concern: the former is responsible for climate change and ocean acidification<sup>14,15</sup>, and the latter causes eutrophication and poses a health risk to drinking water<sup>16</sup>. Developing electrocatalytic reactions based on CO<sub>2</sub> and NO<sub>3</sub><sup>-</sup> could recycle these inorganic wastes as synthons and convert them into useful products under mild conditions. These reactions can also be coupled with electricity generated from renewable energy sources to reduce the carbon footprint.

While CO<sub>2</sub> and NO<sub>3</sub><sup>-</sup> reduction reactions have largely been studied separately thus far, occasional co-reduction experiments have yielded urea as a product<sup>17,18</sup>, demonstrating the potential for generating organonitrogen compounds. However, more advanced catalytic processes are still needed to expand the scope of this reaction to more valuable products such as alkylamines. As the simplest of these, methylamine, which is produced from fossil-fuel-derived methanol (CH<sub>3</sub>OH) and NH<sub>3</sub> under high-temperature high-pressure conditions in the chemical industry (Fig. 1a), is an important building block for valuable chemicals including pharmaceuticals and agrochemicals<sup>19</sup>. The electrochemical reduction of CO<sub>2</sub> and NO<sub>3</sub><sup>-</sup> as C and N sources may afford a greener process to produce methylamine and other related organonitrogen compounds. One big challenge along the route of synthesis is the design of a C–N coupling step to interconnect the separate reduction pathways of the two precursors, which has not been resolved to date.

Here we report a game-changing step on the way to this goal with the discovery of a cascade electrochemical reaction that yields methylamine from the co-reduction of CO<sub>2</sub> and NO<sub>3</sub><sup>-</sup> in aqueous media catalysed by a molecular cobalt catalyst heterogenized on carbon nanotubes (Fig. 1b). Under ambient conditions, methylamine is

generated in a highly cooperative one-pot process that involves the transfer of total of 14 electrons and 15 protons per product molecule. The process has an overall Faradaic efficiency (FE) of 13% and shows no performance decay for at least 16 h of continuous operation, giving a total turnover number (TON) larger than 5,500. We further show that the methylamine is formed in an unprecedented cascade of eight reaction steps on a single electrocatalyst, where the key C–N coupling step is the migration of hydroxylamine (NH<sub>2</sub>OH) from NO<sub>3</sub><sup>-</sup> reduction to spontaneously condense with formaldehyde (HCHO) from CO<sub>2</sub> reduction to form formaldoxime as a key intermediate on the way to methylamine.

## Results

Recently, we developed a cobalt  $\beta$ -tetraaminophthalocyanine/carbon nanotube (CoPc-NH<sub>2</sub>/CNT) hybrid material as the first molecular electrocatalyst that can stably reduce CO<sub>2</sub> first to carbon monoxide (CO) and then to CH<sub>3</sub>OH in substantial yield<sup>6</sup>. The same catalyst is also found to be active for the electroreduction of NO<sub>3</sub><sup>-</sup> to NH<sub>3</sub> with nitrite (NO<sub>2</sub><sup>-</sup>) and NH<sub>2</sub>OH as intermediate products (Extended Data Figs. 1 and 2), consistent with the reported reactivity of metal phthalocyanines towards electrochemical NO<sub>3</sub><sup>-</sup> reduction<sup>10</sup>. This result not only indicates the potential of electrochemical NO<sub>3</sub><sup>-</sup> decomposition or removal from water, which could mitigate the related health and environmental issues, but also implies the possibility of further utilizing the NO<sub>3</sub><sup>-</sup> reduction process to access more complex and valuable products than NH<sub>3</sub>. Considering that both reactions involve the transfer of multiple electrons and protons to the reactants and that the reduction processes both go through a series of intermediates, we thought that deeply reduced products having C–N bonds can be formed if the reduction of CO<sub>2</sub> and NO<sub>3</sub><sup>-</sup> catalysed by CoPc-NH<sub>2</sub>/CNT is performed together in the same reaction mixture.

**Co-reduction of CO<sub>2</sub> and NO<sub>3</sub><sup>-</sup> to methylamine.** Using carbon fibre paper coated with CoPc-NH<sub>2</sub>/CNT as working electrodes

<sup>1</sup>Department of Chemistry, Yale University, New Haven, CT, USA. <sup>2</sup>Energy Sciences Institute, Yale University, West Haven, CT, USA. <sup>3</sup>Department of Materials Science and Engineering, Southern University of Science and Technology, Shenzhen, China. <sup>4</sup>These authors contributed equally: Yueshen Wu, Zhan Jiang, Zhichao Lin. ✉e-mail: [liangyy@sustech.edu.cn](mailto:liangyy@sustech.edu.cn); [hailiang.wang@yale.edu](mailto:hailiang.wang@yale.edu)

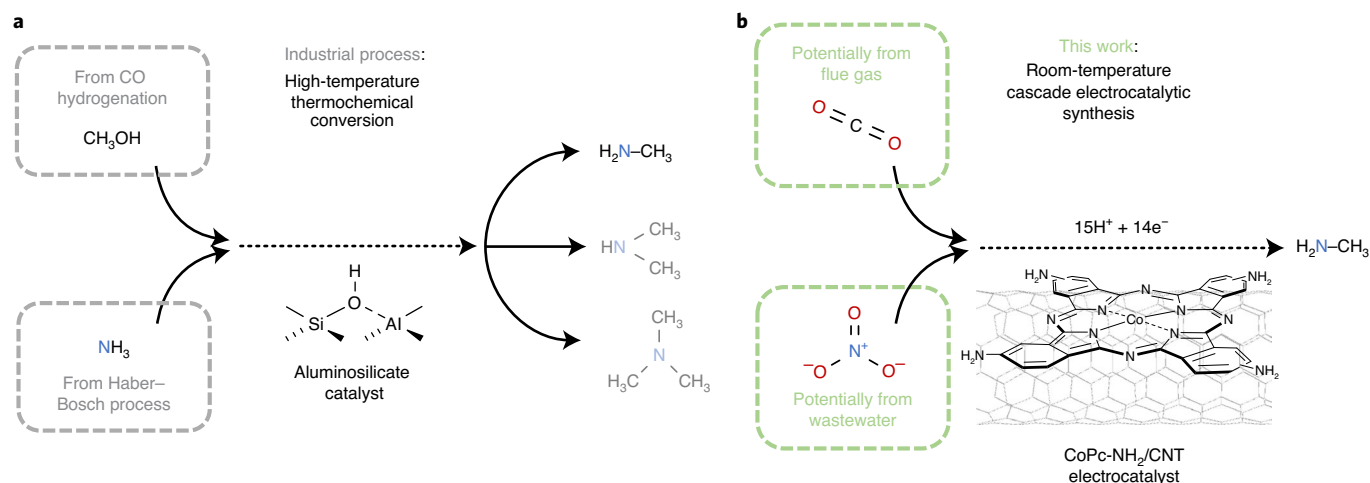


**Fig. 1 | Cascade electrocatalytic synthesis of methylamine from  $\text{CO}_2$  and  $\text{NO}_3^-$ .** **a**, Industrial synthesis of methylamine from fossil fuel feedstocks at high temperature and high pressure. **b**, One-pot electrosynthesis of methylamine from inorganic wastes at ambient temperature and pressure.

and a  $\text{CO}_2$ -saturated aqueous solution containing **0.1 M  $\text{KHCO}_3$**  and **0.5 M  $\text{KNO}_3$**  as electrolyte, **30 min electrolyses** were carried out at various electrode potentials where both  $\text{CO}_2$  reduction to  $\text{CH}_3\text{OH}$  and  $\text{NO}_3^-$  reduction to  $\text{NH}_3$  occur. Gaseous products in the headspace of the electrochemical cell were quantified by gas chromatography (Extended Data Fig. 1). The electrolyte solution was analysed after each electrocatalysis using nuclear magnetic resonance (NMR) and colorimetric methods for quantifying products dissolved in the liquid phase. Interestingly, methylamine is identified as a product, in addition to the common  $\text{CO}_2$  or  $\text{NO}_3^-$  reduction products such as  $\text{CO}$ ,  $\text{CH}_3\text{OH}$ ,  $\text{NO}_2^-$ ,  $\text{NH}_2\text{OH}$  and  $\text{NH}_3$ . Both the singlet at  $\sim 2.61$  ppm in the  $^1\text{H}$  NMR spectrum and the peak at  $\sim 24.8$  ppm in the  $^{13}\text{C}$  NMR spectrum of the electrolyte solution after electrolysis (Fig. 2a) match those of methylamine (Extended Data Fig. 3). The production of methylamine is further confirmed with gas chromatography–mass spectrometry (GC–MS) measurement of a toluene extract of the electrolyte solution that has been treated with pivalic acid anhydride to convert methylamine to organophilic *N*-methylpivalamide (Fig. 2a and Extended Data Fig. 4a)<sup>20</sup>. At  **$-0.92$  V** versus the reversible hydrogen electrode (RHE), **methylamine is produced at the optimal overall FE of 13% with a partial current density of  $3.4 \text{ mA cm}^{-2}$**  (Fig. 2b and Extended Data Fig. 5). This is the first time that methylamine has been synthesized by the electrocatalytic co-reduction of  $\text{CO}_2$  and  $\text{NO}_3^-$ . In prior work, C–N coupling during the electrochemical reduction of inorganic reagents has only formed amides, such as urea from  $\text{CO}_2$  reacting with  $\text{NO}_3^-$  or  $\text{N}_2$  reduction intermediates<sup>17,18,21</sup> or acetamide from  $\text{NH}_3$  reacting with  $\text{CO}$  reduction intermediates<sup>22</sup>. The probable precursors to **methylamine, formaldoxime and *N*-methylhydroxylamine**, are also generated in our system (Extended Data Fig. 3), albeit with FEs lower than 6% and 1%, respectively. Control experiments using  **$^{13}\text{C}$ -labelled  $\text{CO}_2$**  and  **$^{15}\text{N}$ -labelled  $\text{NO}_3^-$**  further confirm that  $\text{CO}_2$  and  $\text{NO}_3^-$  are indeed the C and N sources of these organonitrogen products (Extended Data Fig. 4b,c). Prolonged electrolysis shows that the catalytic performance of  $\text{CoPc-NH}_2/\text{CNT}$  for the electrosynthesis of methylamine can be maintained for at least **16 h** without notable decay, affording an average **FE of 12% and a total TON of 5,600** (counting all the  $\text{CoPc-NH}_2$  molecules loaded on the electrode as active sites;  $\sim 18 \text{ nmol cm}^{-2}$ ) or **10,000** (based on the number of electrochemically active  $\text{CoPc-NH}_2$  molecules determined from cyclic voltammetry;  $\sim 10 \text{ nmol cm}^{-2}$ ; Extended Data Fig. 6).

**Identification of reaction pathway.** To elucidate the mechanistic reaction pathway in which **14 electrons and 15 protons** are transferred to  $\text{CO}_2$  and  $\text{NO}_3^-$  to form methylamine, we first examined the possibility of  $\text{NH}_3$  reacting with  $\text{CO}_2$  reduction intermediates on the basis of the following considerations: (1)  $\text{NH}_3$  is the major product of  $\text{NO}_3^-$  reduction (Extended Data Fig. 2) and is also produced with substantial selectivity in the present co-reduction (Fig. 2b); (2)  $\text{HCHO}$  is probably an active reaction intermediate in the electrochemical reduction of  $\text{CO}_2$  to  $\text{CH}_3\text{OH}$  catalysed by  $\text{CoPc}$  (ref. 23); (3) methylamine can be synthesized from the reaction of  $\text{HCHO}$  with  $\text{NH}_4\text{Cl}$  (ref. 24); and (4) a recent study has shown that  $\text{NH}_3$  can couple with a proposed ketene intermediate from  $\text{CO}$  electroreduction on  $\text{Cu}$  to form acetamide<sup>22</sup>. We first carried out  $\text{CO}_2$  reduction in the presence of  $\text{NH}_4^+$  as the N source (50 mM where  $\text{NH}_4^+$  is the dominant form of ammonia in the  $\text{CO}_2$ -saturated  $\text{KHCO}_3$  solution). No methylamine was detected after the electrolysis (Table 1, Entry 1 and Extended Data Fig. 7a). Electrolysis using  $\text{CO}$  and  $\text{NH}_3$  (2 M  $\text{NH}_4\text{OH}$ ) in a 0.1 M  $\text{KOH}$  solution also failed to produce any methylamine, whereas the co-reduction of  $\text{CO}$  and  $\text{NO}_3^-$  in 0.1 M  $\text{KOH}$  did result in methylamine formation (Table 1, Entries 2 and 3 and Extended Data Fig. 7b). Note that  $\text{CO}$  reduction in alkaline electrolytes is known to occur at considerably more positive potentials on the RHE scale than that in neutral electrolytes<sup>23,25</sup>. These experiments rule out any direct involvement of  $\text{NH}_3$  in the C–N bond formation step that eventually leads to the formation of methylamine and indicate that the reaction pathway in our system is demonstrably different from the reported C–N coupling cases resulting in the formation of urea or acetamide<sup>17,18,22</sup>.

We then performed more systematic control experiments to identify the reaction intermediates responsible for the C–N coupling. Since the co-reduction of  $\text{CO}_2$  and  $\text{NO}_3^-$  in a phosphate buffered solution (PBS) (0.1 M, pH = 6.8) can also form methylamine (Table 1, Entry 4 and Extended Data Fig. 7c), PBS was used in the subsequent control experiments to exclude any potential C or N source from the supporting electrolyte. We used  $\text{NO}_2^-$ ,  $\text{NO}$  or  $\text{NH}_2\text{OH}$ , all of which have been identified as reaction intermediates in the electrochemical reduction of  $\text{NO}_3^-$  to  $\text{NH}_3$  (refs. 26,27), as the N source for co-reduction with  $\text{CO}_2$ . The three experiments all produced methylamine (Table 1, Entries 5–7 and Extended Data Fig. 7c). Among all the N species that can result in methylamine formation when co-reduced with  $\text{CO}_2$ ,  $\text{NH}_2\text{OH}$  is the most reduced intermediate along the reaction pathway of  $\text{NO}_3^-$  reduction to  $\text{NH}_3$  as well as being the most nucleophilic species of those plausibly formed.

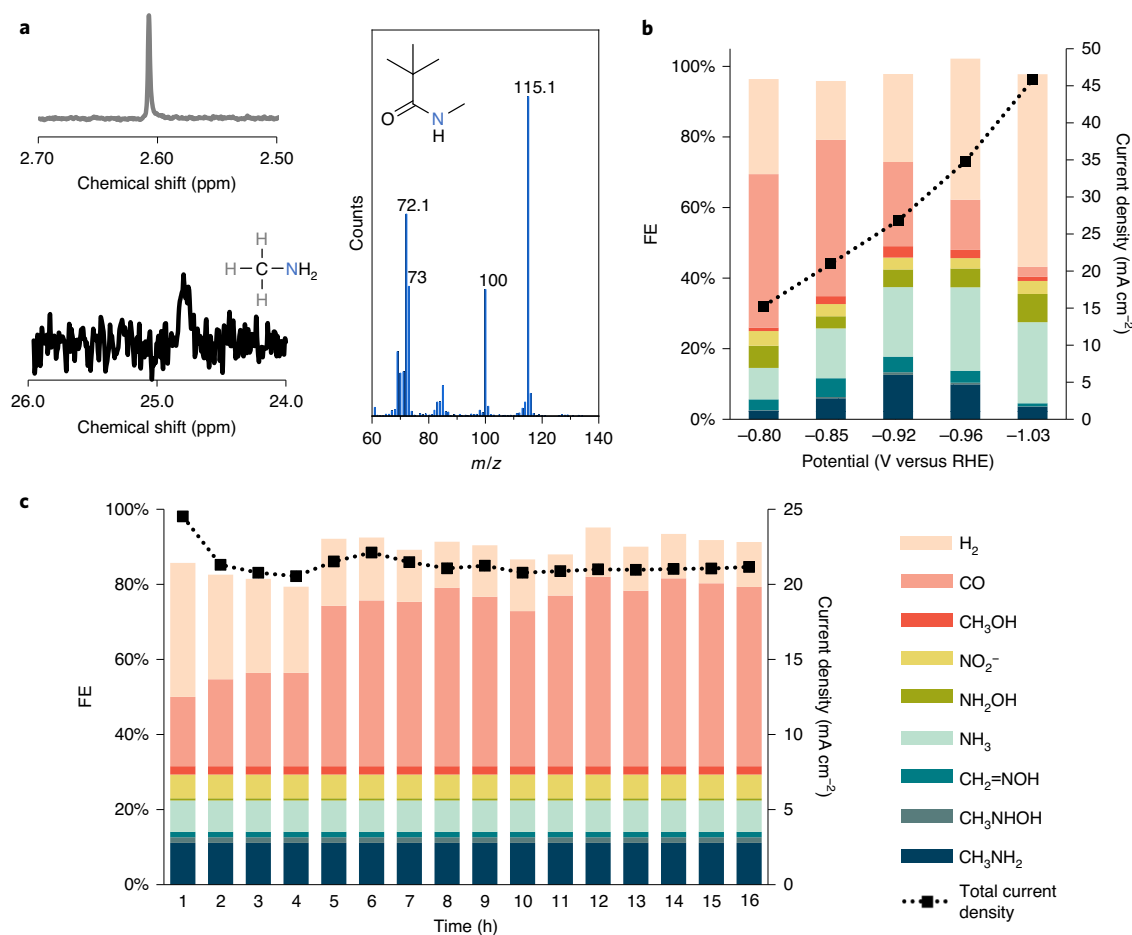


**Fig. 2 | Electrochemical performance of CoPc-NH<sub>2</sub>/CNT for the co-reduction of CO<sub>2</sub> and NO<sub>3</sub><sup>-</sup>.** **a**, Detection of methylamine by  $^1\text{H}$  NMR,  $^{13}\text{C}$  NMR and GC-MS. **b**, Potential-dependent product distribution (FE) and total current density. **c**, Product distribution and total current density during 16 h electrolysis at  $-0.94$  V versus RHE. The liquid products were quantified after the electrolysis was completed, and their average FE was calculated.

**Table 1 | The list of control experiments carried out to elucidate the mechanistic pathway towards methylamine**

Entry	C source	N source	V versus RHE (duration)	CH <sub>3</sub> NH <sub>2</sub> ?	Electrolyte solution
1	CO <sub>2</sub>	NH <sub>4</sub> <sup>+</sup>	$-0.90$ (1h)	No	50 mM NH <sub>4</sub> HCO <sub>3</sub> + 0.1 M KHCO <sub>3</sub>
2	CO	NH <sub>3</sub>	$-0.64$ (1h)	No	2 M NH <sub>4</sub> OH + 0.1 M KOH
3	CO	NO <sub>3</sub> <sup>-</sup>	$-0.64$ (1h)	Yes	0.5 M KNO <sub>3</sub> + 0.1 M KOH
4	CO <sub>2</sub>	NO <sub>3</sub> <sup>-</sup>	$-0.94$ (1h)	Yes	0.5 M KNO <sub>3</sub> + 0.1 M PBS
5	CO <sub>2</sub>	NO <sub>2</sub> <sup>-</sup>	$-0.92$ (1h)	Yes	30 mM NaNO <sub>2</sub> + 0.1 M PBS
6	CO <sub>2</sub>	NO	$-0.92$ (10h)	Yes	0.1 M PBS
7	CO <sub>2</sub>	NH <sub>2</sub> OH	$-0.90$ (1h)	Yes	10 mM NH <sub>2</sub> OH + 0.1 M PBS
8	CO	NO <sub>3</sub> <sup>-</sup>	$-0.96$ (1h)	Yes	0.1 M PBS + 0.5 M KNO <sub>3</sub>
9	HCHO	NO <sub>3</sub> <sup>-</sup>	$-0.90$ (1h)	Yes	50 mM HCHO + 0.1 M PBS + 0.5 M KNO <sub>3</sub>
10	CH <sub>3</sub> OH	NO <sub>3</sub> <sup>-</sup>	$-0.92$ (1h)	No	0.1 M CH <sub>3</sub> OH + 0.1 M PBS + 0.5 M KNO <sub>3</sub>
11	CH <sub>2</sub> =NOH		$-0.93$ (3h)	Yes	2.5 mM CH <sub>2</sub> =NOH + 0.1 M PBS
12	CH <sub>3</sub> NHOH		$-0.92$ (3h)	Yes	5 mM CH <sub>3</sub> NHOH + 0.1 M PBS

It is therefore likely to be the N species involved in C–N bond formation. A similar set of co-reduction experiments were also carried out with CO or HCHO, which are intermediates along the reaction pathway of CO<sub>2</sub> reduction to CH<sub>3</sub>OH catalysed by CoPc (refs. 6,23), as the C source. Methylamine was detected in both cases, whereas using CH<sub>3</sub>OH as the C source did not yield methylamine (Table 1,

Entries 8–10 and Extended Data Fig. 8c). This suggests that HCHO is the intermediate that reacts with NH<sub>2</sub>OH to form the C–N bond. As is well known, hydroxylamines can readily react with aldehydes or ketones to form oximes<sup>28</sup>. The fact that formaldoxime and its reduced product *N*-methylhydroxylamine are also detected in the reaction mixture supports the proposed pathway. Further control

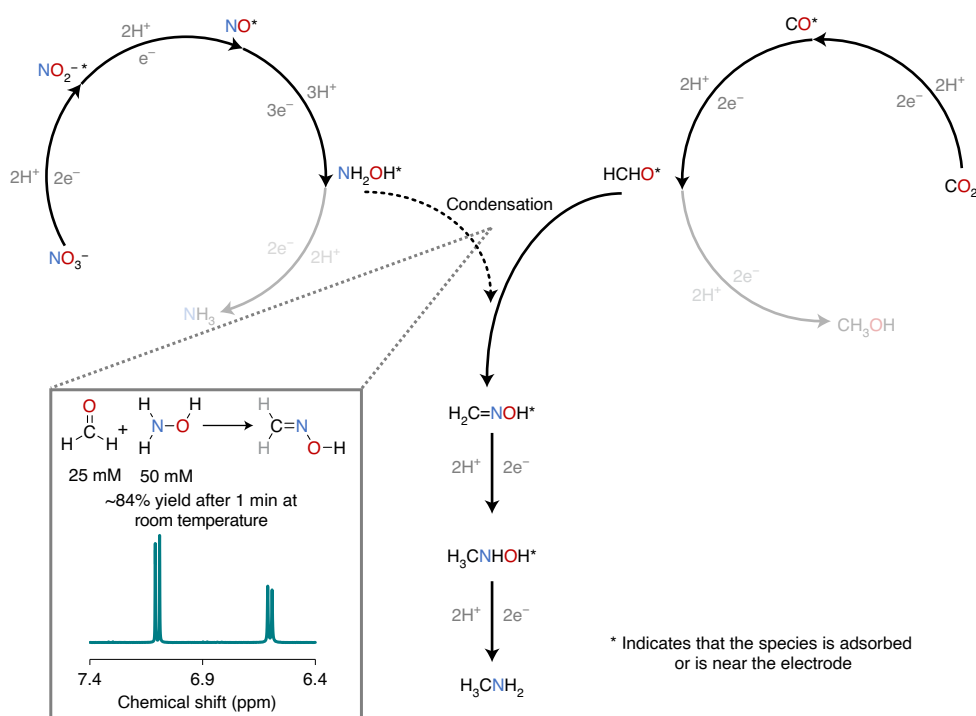


**Fig. 3 |** The proposed reaction pathway of the eight-step cascade electro-synthesis of methylamine from  $\text{CO}_2$  and  $\text{NO}_3^-$  catalysed by  $\text{CoPc-NH}_2/\text{CNT}$ . All the reaction intermediates shown here have been confirmed by experiments. The inset shows the fast kinetics and favourable thermodynamics of the C–N coupling step.

experiments reveal that the electrochemical reduction of formaldoxime or *N*-methylhydroxylamine without other C or N sources can yield methylamine (Table 1, Entries 11 and 12 and Extended Data Fig. 9), consistent with these two co-reduction products being on the reaction pathway to methylamine.

As the C–N coupling step, the spontaneous condensation<sup>29,30</sup> of  $\text{NH}_2\text{OH}$  with  $\text{HCHO}$  to form formaldoxime is the key to the entire catalytic cascade to form methylamine from  $\text{CO}_2$  and  $\text{NO}_3^-$ . In a simple test, we mixed 50 mM  $\text{NH}_2\text{OH}$  and 25 mM  $\text{HCHO}$  in the electrolyte at room temperature and took  $^1\text{H}$  NMR spectra of the mixture after 1 min, which revealed that ~84% of the  $\text{HCHO}$  had already reacted with  $\text{NH}_2\text{OH}$  to form formaldoxime (Fig. 3 and Extended Data Fig. 10a). The fast kinetics and favourable thermodynamics of this reaction ensures effective C–N coupling before the intermediates are further reduced or diffuse into the solution. While only a modest amount of  $\text{NH}_2\text{OH}$  is found among the final products, no trace at all of  $\text{HCHO}$  can be detected by the bisulfite derivatization method (Extended Data Fig. 10b)<sup>31</sup>. This leads us to believe that the coupling step results from the spillover of  $\text{NH}_2\text{OH}$ .

## Discussion

Taken together, the overall reaction scheme can be best described as an unprecedented eight-step electrocatalytic cascade (Fig. 3). Electrochemical  $\text{CO}_2$  reduction and  $\text{NO}_3^-$  reduction first proceed independently until  $\text{HCHO}$  and  $\text{NH}_2\text{OH}$  are formed. Adsorbed  $\text{HCHO}$  then quickly undergoes nucleophilic attack by  $\text{NH}_2\text{OH}$ , yielding formaldoxime, which is further electrochemically reduced to *N*-methylhydroxylamine and then to methylamine.

This reaction demonstrates the direct electro-synthesis of methylamine from  $\text{CO}_2$  and  $\text{NO}_3^-$ . It provides an example of the valorization of chemical species in the atmosphere and water that are of environmental concern.  $\text{NO}_2^-$  and nitrogen oxides, which are also known pollutants, can replace  $\text{NO}_3^-$  as the N source. Methylamine is a feedstock for more complex organic compounds, and this

reaction could therefore be utilized to benefit the sustainable synthesis of many valuable chemicals. The electrochemical method affords not only mild reaction conditions but also the potential for carbon-neutral operation.

The mechanistic understanding of this cascade catalysis will allow us to further optimize the catalytic efficacy by balancing the reaction kinetics of different steps. More excitingly, it will allow us to electrochemically synthesize other, more complex organonitrogen compounds from cheap inorganic source materials by exploiting the key hydroxylamine–carbonyl C–N coupling reaction. For example, we predict that ethylamine and propylamine can be generated from  $\text{CO}_2$  and  $\text{NO}_3^-$  co-reduction catalysed by Cu-based materials; we may also replace  $\text{NO}_3^-$  with the cheaper and more abundant  $\text{N}_2$  as the N source if we find appropriate catalysts that can effectively reduce  $\text{N}_2$  to coupling-active intermediates such as  $\text{NH}_2\text{OH}$ .

## Methods

**Materials.** All chemicals were purchased and used as received without further purification unless otherwise stated.  $\text{CO}_2$  (99.99% or 99.999%),  $\text{CO}$  (99.3% or 99.999%), Ar (99.999%) and  $\text{NO}$  (99.9%) were purchased from Airgas and Huashidai Gas.  $\text{KHCO}_3$  (99.7%) and paraformaldehyde (powder, 95%) were purchased from Sigma-Aldrich.  $\text{KNO}_3$  (99%) and  $\text{NaNO}_2$  (99%) were purchased from Alfa Aesar. PBS (0.1 M) and KOH (99.999%, trace metal basis) were purchased from Aladdin. Ammonium hydroxide solution (30 wt%), ammonium bicarbonate (99%) and hydroxylamine hydrochloride ( $\geq 99\%$ ) were purchased from Acros. Formaldoxime hydrochloride ( $\geq 95\%$ ) and *N*-methylhydroxylamine ( $\geq 98\%$ ) were purchased from Accela. Deionized water used throughout all experiments was purified through either a Pall or a Millipore water purification system to reach a resistivity of 18.2 M $\Omega$  cm (at 25 °C).

**Characterization.** UV–Vis absorption measurements were carried out with a Shimadzu UV–Vis spectrophotometer 3600. Inductively coupled plasma–mass spectrometry (ICP–MS) was performed with an Agilent Technologies 7700 series instrument.  $^1\text{H}$  and  $^{13}\text{C}$  NMR were recorded on a Bruker 400M NMR instrument. GC–MS was measured on an Agilent 5977A mass spectrometer with an Agilent Technologies 7890B GC system.

**Preparation of CoPc-NH<sub>2</sub>/CNT electrodes.** The purification of as-received multiwalled CNTs (FT 9100, C-Nano), the synthesis of CoPc-NH<sub>2</sub> and the hybridization of CoPc-NH<sub>2</sub> with purified CNTs were all carried out as detailed in our previous work, where complementary structural characterization results of the catalyst are available<sup>6</sup>. The weight percentage of CoPc-NH<sub>2</sub> in the hybrid material is ~2.9%, as derived from ICP-MS measurements. Catalyst ink was prepared by dispersing 2 mg of CoPc-NH<sub>2</sub>/CNT in 2 ml of ethanol with 6 µl of 5 wt% Nafion solution followed by sonication for 1 h. Then, 200 µl of the ink was drop-casted onto a 3 × 0.5 cm<sup>2</sup> polytetrafluoroethylene-treated carbon fibre paper (Toray 030, Fuel Cell Store) to cover a 0.5 × 1 cm<sup>2</sup> area (catalyst mass loading, 0.4 mg cm<sup>-2</sup>). The prepared electrodes were dried using an infrared lamp.

**Preparation of electrolyte solutions.** The supporting electrolyte solutions used in this study (KHCO<sub>3</sub>, KNO<sub>3</sub>, PBS and KOH) were purified through a column containing ion-exchanged Chelex 100 Resin (sodium form, Sigma-Aldrich) following the manufacturer's protocol with some modifications<sup>32</sup>. To prepare the purification column, 25 g of the as-received resin was dispersed in 100 ml of deionized water, poured into the sand column (inner diameter, 20 mm; height, 300 mm) and then washed with another 100 ml of deionized water. The Na<sup>+</sup> in the resin was exchanged with K<sup>+</sup> by sequentially running the column with 100 ml of 1 M HCl, 200 ml of deionized water, 100 ml of 1 M KOH and finally an ample amount of deionized water until the eluent was pH neutral. For purification, the electrolyte solution was run through the resin-packed column. The first 100 ml was used to displace the residual water in the column and was discarded. The subsequent eluent was then collected as purified electrolyte solution. C sources, N sources and C-N compounds (if in liquid or solid form) in all the control experiments were added to the purified electrolyte solution. For the co-reduction of HCHO and NO<sub>3</sub><sup>-</sup>, paraformaldehyde was dissolved and hydrolysed in the purified electrolyte solution (60 °C, 1 h) to generate HCHO.

**Electrochemical measurements.** Electrolyses were performed using a CHI 660E or a Biologic VMP3 potentiostat and a custom-designed gas-tight two-compartment electrochemical cell. Graphite rod counter electrodes (99.999%) and Ag/AgCl reference electrodes (3 M KCl, 0.210 V versus RHE; saturated calomel electrodes were used instead in KOH) were purchased from Alfa Aesar and Gaoss Union. The cathode compartment and the anode compartment were separated by an **anion exchange membrane** (Selemion DSV). Each compartment contained 13 ml of electrolyte solution. Before each electrolysis, the electrolyte was presaturated with reactant gas or Ar by bubbling the gas for at least 15 min. In all cases, gas was continuously bubbled into the electrolyte during electrolysis at a flow rate of 20 standard cubic centimetres per minute. Before the start of each electrolysis, the **ohmic drop** between the working electrode and the reference electrode was determined using potentiostatic electrochemical impedance spectroscopy at -0.5 V versus Ag/AgCl between 200 kHz and 1 Hz with an amplitude of 10 mV. The resistance value was then determined by the intersection of the curve with the Re (Ω) axis in the Nyquist plot. iR correction was performed after electrolysis for all measurements. **Every measurement was performed on a freshly prepared electrode.** Current densities were calculated on the basis of the catalyst-covered geometric area of the working electrode. All potentials were converted to the RHE scale using the following formula:  $V$  (versus RHE) =  $V$  (versus Ag/AgCl) + 0.210 V + 0.0592 V × pH.

**TON calculation.** TON was reported as the number of methylamine molecules produced in the 16 h electrolysis at -0.94 V (Fig. 2c) per active CoPc-NH<sub>2</sub> molecule. The total number of active CoPc-NH<sub>2</sub> molecules on the electrode was determined using two different methods: (1) counting all the CoPc-NH<sub>2</sub> molecules loaded on the electrode from ICP-MS measurements, and (2) calculating the number of electrochemically active CoPc-NH<sub>2</sub> molecules on the electrode from integrating the **one-electron reduction peak**<sup>33,34</sup> near -0.70 V versus Ag/AgCl in the cyclic voltammogram (Extended Data Fig. 6). Both TON values were reported.

**GC-MS measurements.** Prior to the GC-MS measurement, methylamine in the electrolyte solution after electrolysis was first derivatized into *N*-methylpivalamide. Then, 1 g of potassium carbonate (Aladdin), 3 g of sodium chloride (Aladdin), 0.5 ml of pivalic acid anhydride (Aladdin) and 0.5 ml of toluene (HPLC grade, Sigma-Aldrich) were sequentially added into 10 ml of the electrolyte solution, which was kept at 40 °C in a water bath. The mixture was then subject to vortex mixing (IKA Lab Dancer) for 40 min and rested until phase separation. The top toluene layer was then sampled and injected into the GC-MS system for analysis.

**Product quantification.** The gas products of electrocatalysis were analysed by a gas chromatograph (SRI 8610C) equipped with a flame ionization detector and a thermal conductivity detector. High-purity Ar was used as the carrier gas. The peak areas of the products (H<sub>2</sub> and CO) were converted to gas volumes using calibration curves that were obtained using a standard gas diluted to different concentrations with CO<sub>2</sub>. The FEs of the gas products were reported as the averages of two or three measurements.

The organic products in the reaction mixture were quantified after electrocatalysis by <sup>1</sup>H NMR with solvent (H<sub>2</sub>O) suppression. For electrolysis

without CO<sub>2</sub>, CO<sub>2</sub> was bubbled into the reaction mixture after the electrolysis for at least 10 min to **adjust the pH to near neutral prior to all <sup>1</sup>H NMR measurements** (except for KOH electrolyte samples). Then, 400 µl of electrolyte was mixed with 100 µl of 10 mM potassium benzoate (99%, Alfa Aesar) in D<sub>2</sub>O (99.8 atom%, Acros) as the internal standard for <sup>1</sup>H NMR (parameter: d1 = 20 s; scan number, 32) or <sup>13</sup>C NMR analysis. The concentration of the analyte was calculated on the basis of the area ratio of the analyte peak (methylamine, ~2.61 ppm; CH<sub>3</sub>OH, ~3.35 ppm; formaldoxime (trans H), ~7.10 ppm (ref. 35); *N*-methylhydroxylamine, ~2.72 ppm) to that of the internal standard (2,6-H of benzoate, ~7.80 ppm).

NO<sub>2</sub><sup>-</sup>, NH<sub>2</sub>OH and NH<sub>3</sub> were quantified by long-established colorimetric methods with some modifications. **NO<sub>2</sub><sup>-</sup> was quantified through the Griess test**, where NO<sub>2</sub><sup>-</sup> reacts with 4-aminobenzenesulfonamide and *N*-(1-naphthyl)ethylenediamine in two steps to form a pink-coloured azo compound<sup>36</sup>. In this test, 100 µl of a 4-aminobenzenesulfonamide aqueous solution (10 g l<sup>-1</sup> in 10 wt% HCl, Dongjiang Chemical Reagent) was added into 2 ml of the sample and allowed to react for 8 min; 100 µl of a *N*-(1-naphthyl)ethylenediamine dihydrochloride aqueous solution (1 g l<sup>-1</sup>, Aladdin) was subsequently added and allowed to further react for 10 min. The sample was then taken for UV-Vis absorption measurement within 2 h. A series of standard samples with known [NO<sub>2</sub><sup>-</sup>] (in the KHCO<sub>3</sub> + KNO<sub>3</sub> electrolyte) was prepared and measured to establish the calibration curve (Extended Data Fig. 1b) on the basis of the maximum absorbance at 540 nm. The [NO<sub>2</sub><sup>-</sup>] of an unknown sample was calculated using its absorbance at 540 nm and the calibration curve. The quantification of **NH<sub>2</sub>OH** is based on its reduction of Fe<sup>3+</sup> to Fe<sup>2+</sup>, which then forms an orange complex with 1,10-phenanthroline<sup>37</sup>. 100 µl of an aqueous acetate buffer (1 M sodium acetate + 1 M acetic acid, TCI), 100 µl of a 4 mM ammonium ferric sulfate aqueous solution (Macklin) and 100 µl of a 10 mM 1,10-phenanthroline ethanolic solution (Rhawn) were sequentially added into 3 ml of the sample. A series of standard samples with known [NH<sub>2</sub>OH] (in the KHCO<sub>3</sub> + KNO<sub>3</sub> electrolyte) was prepared and measured to establish the calibration curve (Extended Data Fig. 1d) on the basis of the maximum absorbance at 510 nm. The [NH<sub>2</sub>OH] of an unknown sample was calculated using its absorbance at 510 nm and the calibration curve. **NH<sub>3</sub> was quantified using the salicylate method**, where NH<sub>3</sub> is converted into **indophenol blue** via reaction with salicylate and hypochlorite<sup>38</sup>. In this method, 500 µl of an aqueous solution containing 0.4 M sodium salicylate and 0.32 M sodium hydroxide (Aladdin), 50 µl of a sodium hypochlorite aqueous solution containing ~4.5% active chlorine (Aladdin) and 0.75 M sodium hydroxide, and 50 µl of a sodium nitroferrocyanide aqueous solution (10 mg ml<sup>-1</sup>, Aladdin) were sequentially added to 3 ml of the sample. A series of standard samples with known [NH<sub>4</sub><sup>+</sup>] (in the KHCO<sub>3</sub> + KNO<sub>3</sub> electrolyte) was prepared and measured to establish the calibration curve (Extended Data Fig. 1f) on the basis of the maximum absorbance at 675 nm. The [NH<sub>3</sub>] of an unknown sample was calculated using its absorbance at 675 nm and the calibration curve. A blank sample prepared from a fresh electrolyte solution was measured before every UV-Vis measurement to ensure no major contamination of the electrolyte solution and to serve as the baseline. These colorimetric methods were found to be orthogonal; **the presence of any one of the three species does not have a colorimetric response to the quantification methods for the others.** Formaldoxime was found to slightly interfere with the quantifications of NH<sub>2</sub>OH and NH<sub>3</sub>. To correct for this minor interference, a series of standard formaldoxime hydrochloride solutions with known concentrations was used to establish the calibration curve (absorbance versus concentration):  $A_{510\text{nm}} = 0.0031 \times [\text{formaldoxime}]$  (µM) in the quantification method of NH<sub>2</sub>OH and  $A_{675\text{nm}} = 0.0006 \times [\text{formaldoxime}]$  (µM) in the quantification method of NH<sub>3</sub>. The concentration of formaldoxime present in the sample (as determined by <sup>1</sup>H NMR) was used to calculate the absorbance contribution from formaldoxime, which was then subtracted from the total absorbance value for quantifying NH<sub>2</sub>OH or NH<sub>3</sub>.

The dataset shown in Fig. 2b was selected to represent the catalytic performance of methylamine production (1) near the onset potential, (2) near the optimal potential and (3) at more negative potentials where FE<sub>methylamine</sub> and  $j_{\text{methylamine}}$  decline. Extended Data Fig. 5 shows the distributions of quantified methylamine selectivity (FE<sub>methylamine</sub>) and methylamine partial current density ( $j_{\text{methylamine}}$ ) across the potential range of interest for 27 independent co-electrolyses of CO<sub>2</sub> and NO<sub>3</sub><sup>-</sup>. The entries with 'Yes' in Table 1 signify that the concentration of methylamine in the corresponding cases are at least 0.05 mM after reaction. The entries with 'No' in Table 1 signify that no methylamine peak is present in the <sup>1</sup>H NMR spectra of the reaction mixture.

**Detection of HCHO.** The detection of HCHO in the electrolyte solution after the reaction was performed according to an established method<sup>31</sup>. Freshly prepared aqueous sodium bisulfite (1 M, Aladdin) was vigorously mixed with the sample (50:50, v/v). <sup>1</sup>H NMR measurement of the mixture was then performed. A standard sample of HCHO (in the CO<sub>2</sub>-saturated KHCO<sub>3</sub> + KNO<sub>3</sub> electrolyte) reacts with bisulfite to form **sodium formaldehyde bisulfite**, which has a singlet peak at ~4.39 ppm. In comparison, a mixture of formaldoxime with bisulfite in the same electrolyte gives a singlet peak at ~4.00 ppm (Extended Data Fig. 10b). The post-electrolysis solution of the CO<sub>2</sub> + NO<sub>3</sub><sup>-</sup> co-reduction mixed with sulfite shows the singlet peak near 4.00 ppm but not the one near 4.39 ppm (Extended Data Fig. 10b), ruling out the presence of free HCHO in the product stream.

**Chemical reaction between NH<sub>2</sub>OH and HCHO.** A CO<sub>2</sub>-saturated electrolyte solution (0.1 M KHCO<sub>3</sub> + 0.5 M KNO<sub>3</sub>) containing 25 mM HCHO (from 37 wt% formaldehyde solution, JT Baker) and another CO<sub>2</sub>-saturated electrolyte solution containing 50 mM hydroxylamine hydrochloride were prepared in two separate vials. Then, 225 µl of each solution was sequentially added to an NMR tube containing 50 µl of D<sub>2</sub>O with 10 mM potassium benzoate as the internal standard. The NMR tube was rested for 1 min before <sup>1</sup>H NMR measurement, which took approximately 10 min in total.

### Data availability

The data supporting the findings of this study are available from the corresponding authors upon reasonable request.

Received: 14 January 2021; Accepted: 24 February 2021;

Published online: 05 April 2021

### References

- Resasco, J. & Bell, A. T. Electrocatalytic CO<sub>2</sub> reduction to fuels: progress and opportunities. *Trends Chem.* **2**, 825–836 (2020).
- De Luna, P. et al. What would it take for renewably powered electrosynthesis to displace petrochemical processes? *Science* **364**, eaav3506 (2019).
- Liu, A. et al. Current progress in electrocatalytic carbon dioxide reduction to fuels on heterogeneous catalysts. *J. Mater. Chem. A* **8**, 3541–3562 (2020).
- Jouny, M., Hutchings, G. S. & Jiao, F. Carbon monoxide electroreduction as an emerging platform for carbon utilization. *Nat. Catal.* **2**, 1062–1070 (2019).
- Giddey, S., Badwal, S. P. S. & Kulkarni, A. Review of electrochemical ammonia production technologies and materials. *Int. J. Hydrog. Energy* **38**, 14576–14594 (2013).
- Wu, Y., Jiang, Z., Lu, X., Liang, Y. & Wang, H. Domino electroreduction of CO<sub>2</sub> to methanol on a molecular catalyst. *Nature* **575**, 639–642 (2019).
- Li, F. et al. Cooperative CO<sub>2</sub>-to-ethanol conversion via enriched intermediates at molecule–metal catalyst interfaces. *Nat. Catal.* **3**, 75–82 (2020).
- Liu, Y. et al. Steering CO<sub>2</sub> electroreduction toward ethanol production by a surface-bound Ru polypyridyl carbene catalyst on N-doped porous carbon. *Proc. Natl Acad. Sci. USA* **116**, 26353–26358 (2019).
- Francis, S. A. et al. Reduction of aqueous CO<sub>2</sub> to 1-propanol at MoS<sub>2</sub> electrodes. *Chem. Mater.* **30**, 4902–4908 (2018).
- Chebotaeva, N. & Nyokong, T. Metallophthalocyanine catalysed electroreduction of nitrate and nitrite ions in alkaline media. *J. Appl. Electrochem.* **27**, 975–981 (1997).
- Brylev, O., Sarrazin, M., Roué, L. & Bélanger, D. Nitrate and nitrite electrocatalytic reduction on Rh-modified pyrolytic graphite electrodes. *Electrochim. Acta* **52**, 6237–6247 (2007).
- Wang, Y., Zhou, W., Jia, R., Yu, Y. & Zhang, B. Unveiling the activity origin of a copper-based electrocatalyst for selective nitrate reduction to ammonia. *Angew. Chem. Int. Ed. Engl.* **59**, 5350–5354 (2020).
- McEnaney, J. M. et al. Electrolyte engineering for efficient electrochemical nitrate reduction to ammonia on a titanium electrode. *ACS Sustain. Chem. Eng.* **8**, 2672–2681 (2020).
- IPCC *Climate Change 2014: Synthesis Report* (eds Core Writing Team, Pachauri, R. K. & Meyer, L. A.) (IPCC, 2014).
- Doney, S. C., Fabry, V. J., Feely, R. A. & Kleypas, J. A. Ocean acidification: the other CO<sub>2</sub> problem. *Annu. Rev. Mar. Sci.* **1**, 169–192 (2009).
- Ward, M. H. et al. Drinking water nitrate and human health: an updated review. *Int. J. Environ. Res. Public Health* **15**, 1557 (2018).
- Shibata, M., Yoshida, K. & Furuya, N. Electrochemical synthesis of urea on reduction of carbon dioxide with nitrate and nitrite ions using Cu-loaded gas-diffusion electrode. *J. Electroanal. Chem.* **387**, 143–145 (1995).
- Shibata, M. & Furuya, N. Electrochemical synthesis of urea at gas-diffusion electrodes: Part VI. Simultaneous reduction of carbon dioxide and nitrite ions with various metallophthalocyanine catalysts. *J. Electroanal. Chem.* **507**, 177–184 (2001).
- Corbin, D. R., Schwarz, S. & Sonnichsen, G. C. Methylamines synthesis: a review. *Catal. Today* **37**, 71–102 (1997).
- Joppich, M., Joppich-Kühn, R., Sentissi, A. & Giese, R. W. Single-step, quantitative derivatization of amino, carboxyl, and hydroxyl groups in iodothyronine amino acids with ethanolic pivalic anhydride containing 4-dimethylaminopyridine. *Anal. Biochem.* **153**, 159–165 (1986).
- Chen, C. et al. Coupling N<sub>2</sub> and CO<sub>2</sub> in H<sub>2</sub>O to synthesize urea under ambient conditions. *Nat. Chem.* **12**, 717–724 (2020).
- Jouny, M. et al. Formation of carbon–nitrogen bonds in carbon monoxide electrolysis. *Nat. Chem.* **11**, 846–851 (2019).
- Boutin, E. et al. Aqueous electrochemical reduction of carbon dioxide and carbon monoxide into methanol with cobalt phthalocyanine. *Angew. Chem. Int. Ed. Engl.* **58**, 16172–16176 (2019).
- Marvel, C. S. & Jenkins, R. L. Methylamine hydrochloride. *Organic Synth.* **3**, 67 (1923).
- Wu, Y., Hu, G., Rooney, C. L., Brudvig, G. W. & Wang, H. Heterogeneous nature of electrocatalytic CO/CO<sub>2</sub> reduction by cobalt phthalocyanines. *ChemSusChem* **13**, 6296–6299 (2020).
- Duca, M. & Koper, M. T. M. Powering denitrification: the perspectives of electrocatalytic nitrate reduction. *Energy Environ. Sci.* **5**, 9726–9742 (2012).
- García-Segura, S., Lanzarini-Lopes, M., Hristovski, K. & Westerhoff, P. Electrocatalytic reduction of nitrate: fundamentals to full-scale water treatment applications. *Appl. Catal. B* **236**, 546–568 (2018).
- Rosenberg, S., Silver, S. M., Sayer, J. M. & Jencks, W. P. Evidence for two concurrent mechanisms and a kinetically significant proton transfer process in acid-catalyzed O-methylxime formation. *J. Am. Chem. Soc.* **96**, 7986–7998 (1974).
- Wu, Z., Liang, H. & Lu, J. Synthesis of poly(N-isopropylacrylamide)–poly(ethylene glycol) miktoarm star copolymers via RAFT polymerization and aldehyde–aminoxy click reaction and their thermoinduced micellization. *Macromolecules* **43**, 5699–5705 (2010).
- Hudak, J. E. et al. Synthesis of heterobifunctional protein fusions using copper-free click chemistry and the aldehyde tag. *Angew. Chem. Int. Ed. Engl.* **51**, 4161–4165 (2012).
- Chatterjee, T., Boutin, E. & Robert, M. Manifesto for the routine use of NMR for the liquid product analysis of aqueous CO<sub>2</sub> reduction: from comprehensive chemical shift data to formaldehyde quantification in water. *Dalton Trans.* **49**, 4257–4265 (2020).
- Chelex® 100 and Chelex 20 Chelating Ion Exchange Resin Instruction Manual* (Bio-Rad, 2000).
- Irvine, J. T. S., Eggins, B. R. & Grimshaw, J. The cyclic voltammetry of some sulphonated transition metal phthalocyanines in dimethylsulphoxide and in water. *J. Electroanal. Chem. Interf. Electrochem.* **271**, 161–172 (1989).
- Lieber, C. M. & Lewis, N. S. Catalytic reduction of carbon dioxide at carbon electrodes modified with cobalt phthalocyanine. *J. Am. Chem. Soc.* **106**, 5033–5034 (1984).
- Jensen, K. A., Holm, A. & Andersen, F. A. *Investigations of Formaldehyde Oxime, Its Polymers and Coordination Compounds* Vol. 1 (Kongelige Danske Videnskabernes Selskab, 1978).
- Snell, F. D. & Snell, C. T. *Colorimetric Methods of Analysis* (D. van Nostrand, 1959).
- Fortune, W. B. & Mellon, M. G. Determination of iron with o-phenanthroline: a spectrophotometric study. *Ind. Eng. Chem. Anal. Ed.* **10**, 60–64 (1938).
- Bower, C. E. & Holm-Hansen, T. A salicylate–hypochlorite method for determining ammonia in seawater. *Can. J. Fish. Aquat. Sci.* **37**, 794–798 (1980).

### Acknowledgements

The work at Yale was supported by the US National Science Foundation (grant no. CHE-1651717). The work at Southern University of Science and Technology was supported by the National Science Foundation of China (grant no. 22075125). Y.W. acknowledges the Dox Fellowship from Yale University. H.W. acknowledges the Sloan Research Fellowship.

### Author contributions

Y.W. and H.W. conceived the project and designed the experiments. Y.W., Z.J. and Z.L. performed the experiments and analysed the data with input from Y.L. and H.W. Y.W. and H.W. wrote the manuscript with input from all other authors. Y.L. and H.W. supervised the project.

### Competing interests

The authors declare no competing interests.

### Additional information

**Extended data** is available for this paper at <https://doi.org/10.1038/s41893-021-00705-7>.

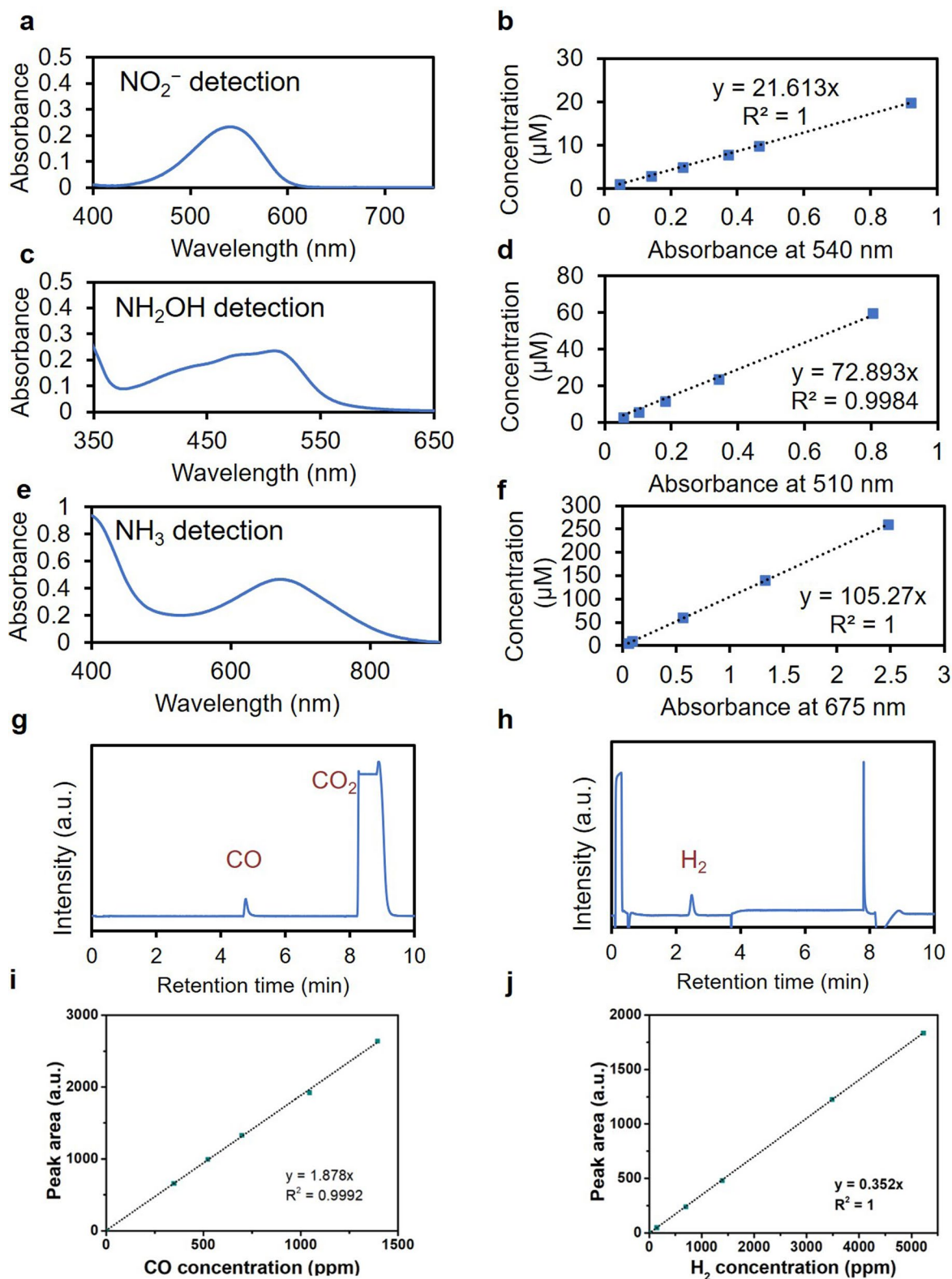
**Correspondence and requests for materials** should be addressed to Y.L. or H.W.

**Peer review information** *Nature Sustainability* thanks Feng Jiao and the other, anonymous, reviewer(s) for their contribution to the peer review of this work.

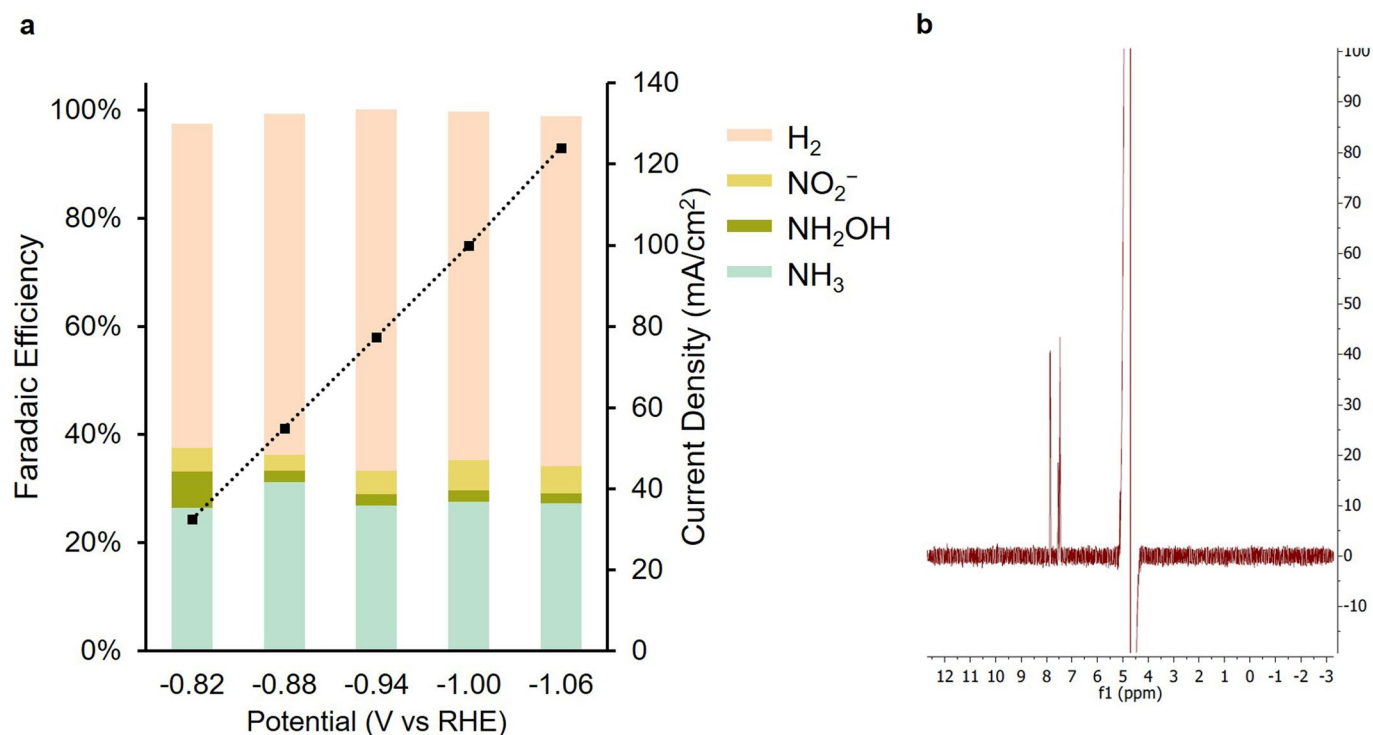
**Reprints and permissions information** is available at [www.nature.com/reprints](http://www.nature.com/reprints).

**Publisher's note** Springer Nature remains neutral with regard to jurisdictional claims in published maps and institutional affiliations.

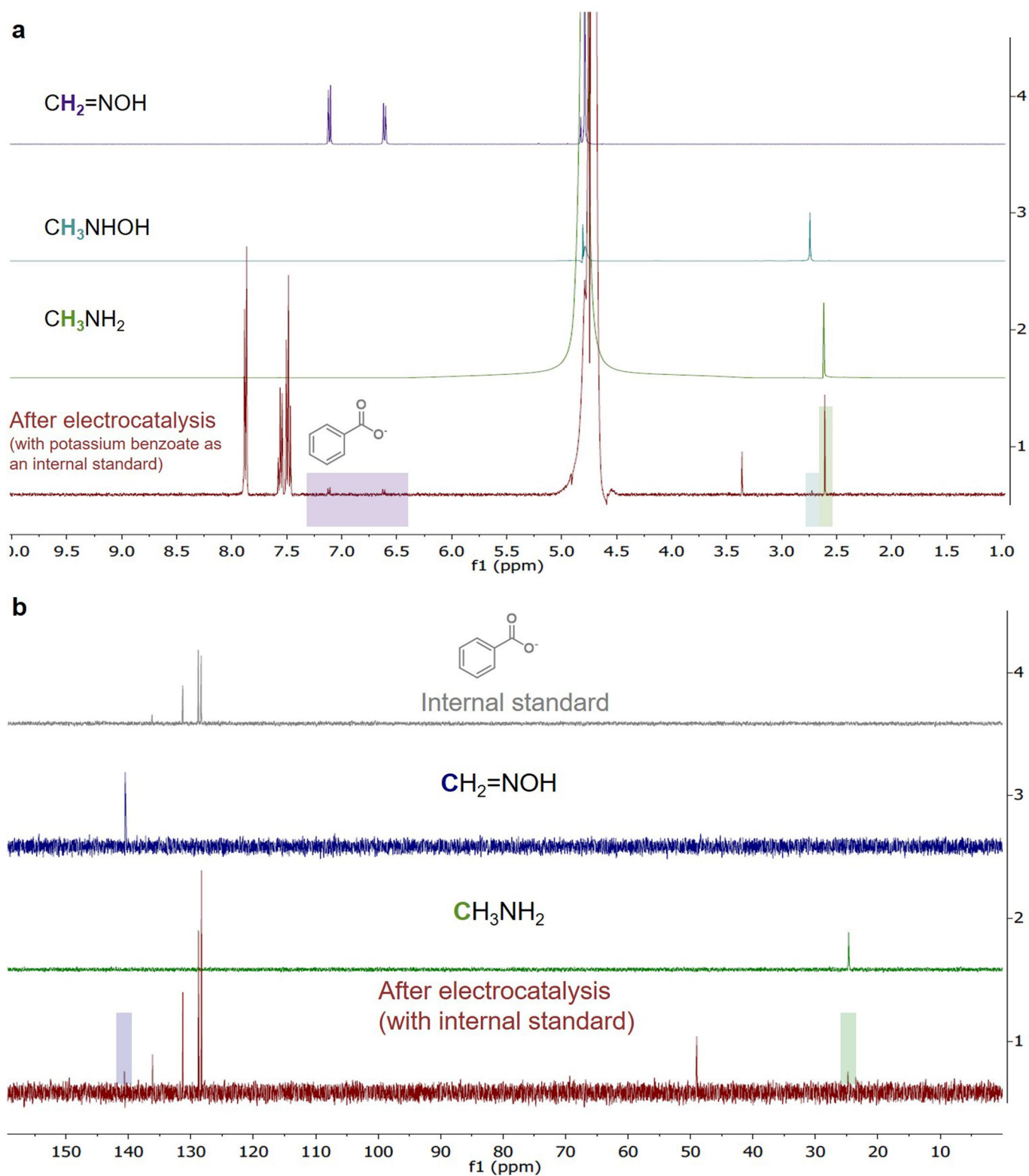
© The Author(s), under exclusive licence to Springer Nature Limited 2021



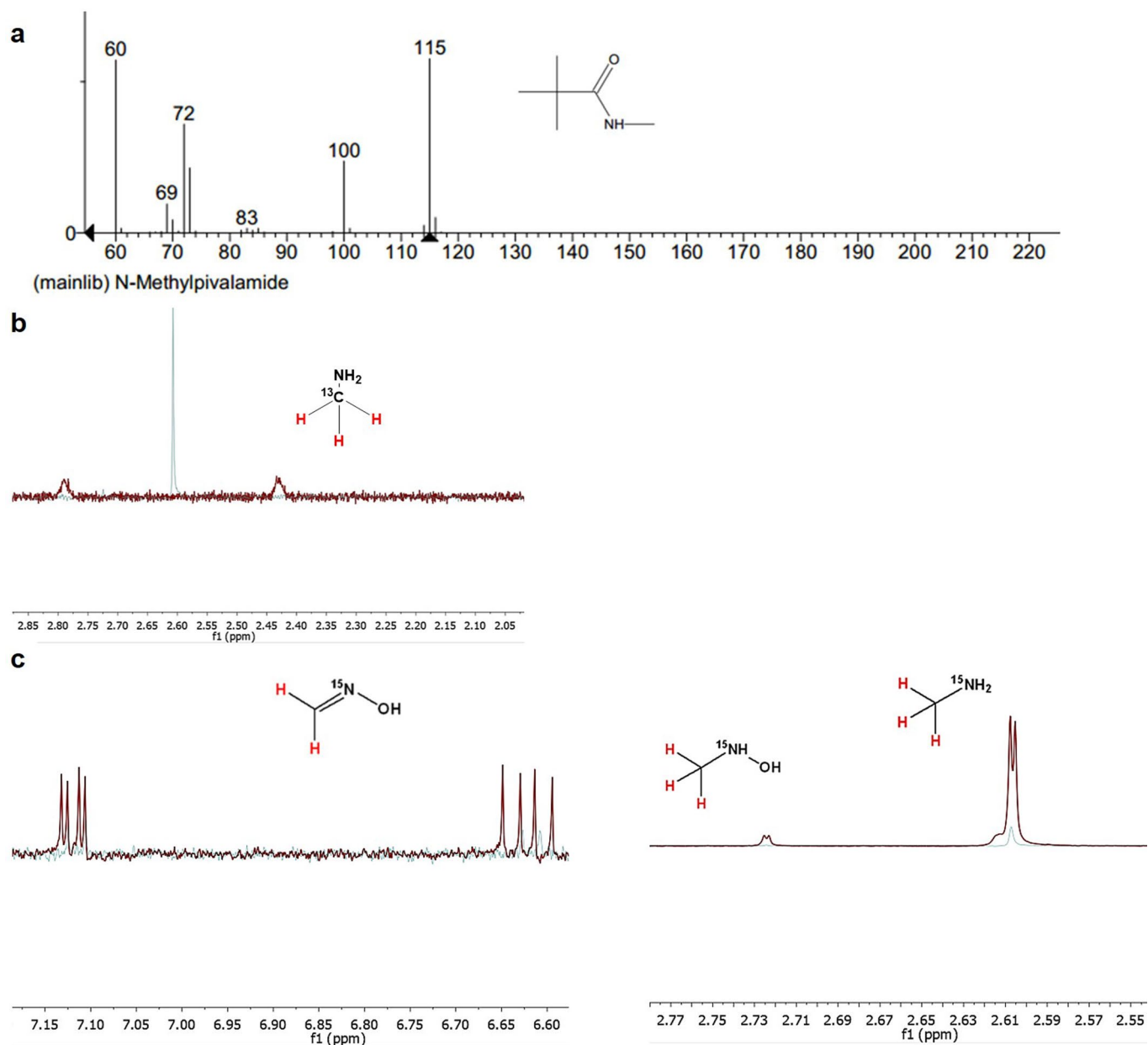
**Extended Data Fig. 1 | Liquid-phase and gas-phase product quantification.** UV-vis spectra and calibration curves (with linear fitting equations and  $R^2$  values) for colorimetric quantification of **a,b**,  $\text{NO}_2^-$ , **c,d**,  $\text{NH}_2\text{OH}$  and **e,f**,  $\text{NH}_3$ . Typical gas chromatography diagrams from **g**, the flame ionization detector and **h**, the thermal conductivity detector, showing the presence of  $\text{CO}$ ,  $\text{CO}_2$  and  $\text{H}_2$ . Calibration curves for **i**,  $\text{CO}$  and **j**,  $\text{H}_2$ .



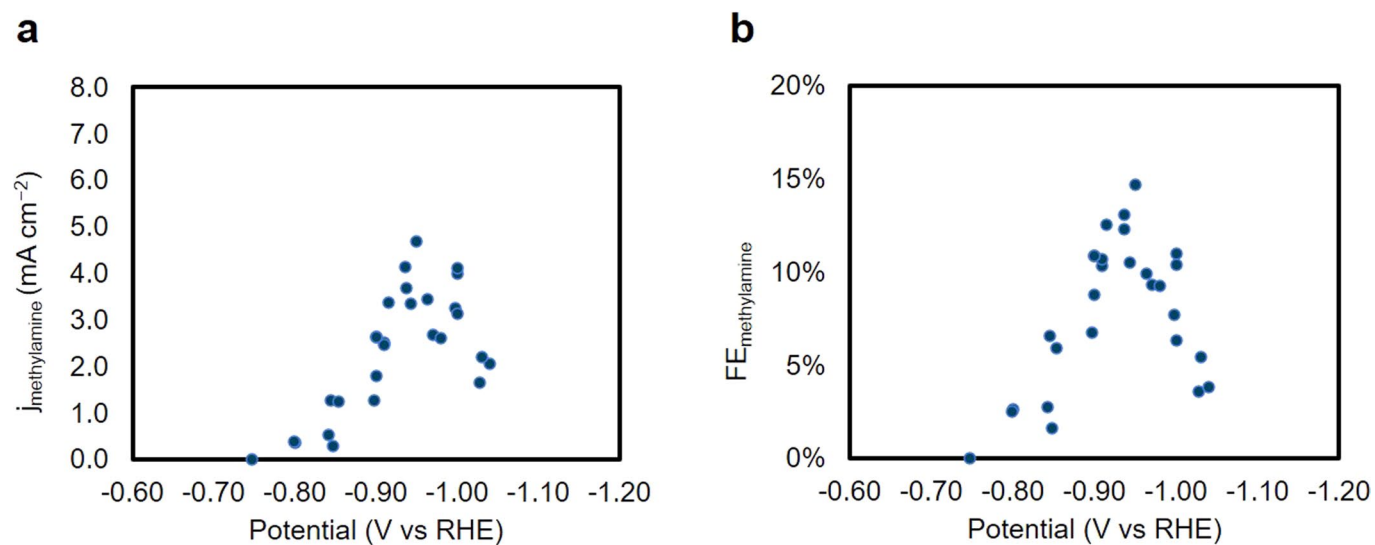
**Extended Data Fig. 2 | Electrochemical NO<sub>3</sub><sup>-</sup> reduction catalyzed by CoPc-NH<sub>2</sub>/CNT. **a**, Potential-dependent product selectivity and current density of electrochemical NO<sub>3</sub><sup>-</sup> reduction catalyzed by CoPc-NH<sub>2</sub>/CNT. 24 min electrolyses were carried out in an Ar-saturated aqueous solution containing 0.1M PBS and 0.5 M KNO<sub>3</sub>. **b**, <sup>1</sup>H NMR spectrum of the catholyte solution after electrochemical NO<sub>3</sub><sup>-</sup> reduction at -0.94 V.**



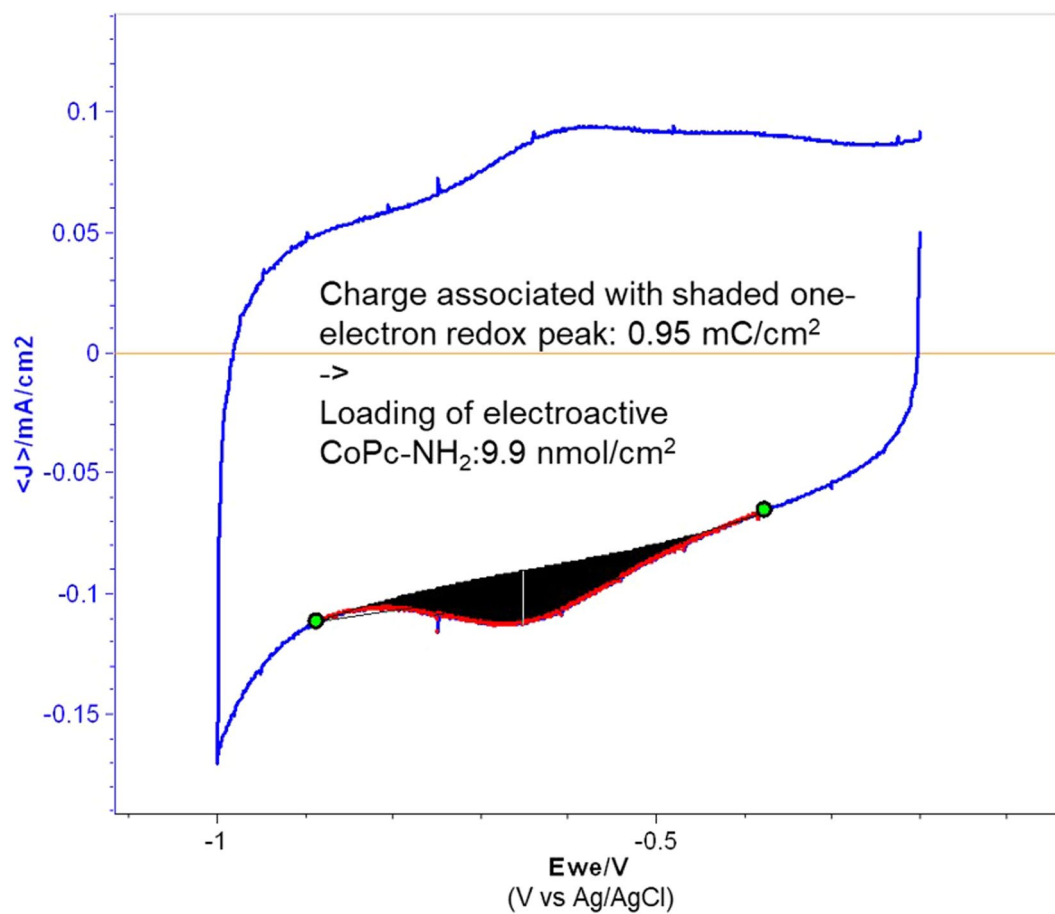
**Extended Data Fig. 3 | Identification of liquid-phase products from co-reduction in NMR spectra.** Typical **a**,  $^1\text{H}$  NMR and **b**,  $^{13}\text{C}$  NMR spectra of the catholyte solution after co-reduction stacked together with standard spectra of methylamine, N-methylhydroxylamine and formaldoxime dissolved in fresh  $\text{CO}_2$ -saturated electrolyte solutions.



**Extended Data Fig. 4 | Further confirmation of methylamine formation and its C, N sources. a**, Standard mass spectrum of N-methylpivalamide from NIST Mass Spectral Library. **b**,  $^1\text{H}$  NMR spectrum of methylamine after electrolysis in 0.1M PBS + 0.5M  $\text{KNO}_3$  under  $^{13}\text{CO}_2$  for 30 min at  $-0.95$  V vs RHE. **c**,  $^1\text{H}$  NMR spectrum of formaldoxime, N-methylhydroxylamine and methylamine after electrolysis in 0.1M  $\text{KHCO}_3$  + 0.5M  $\text{K}^{15}\text{NO}_3$  under  $\text{CO}_2$  for 5 h at  $-0.91$  V vs RHE. The green traces show the  $^1\text{H}$  NMR spectra of formaldoxime, N-methylhydroxylamine and methylamine from co-reduction of unlabeled  $\text{CO}_2$  and  $\text{NO}_3^-$ .

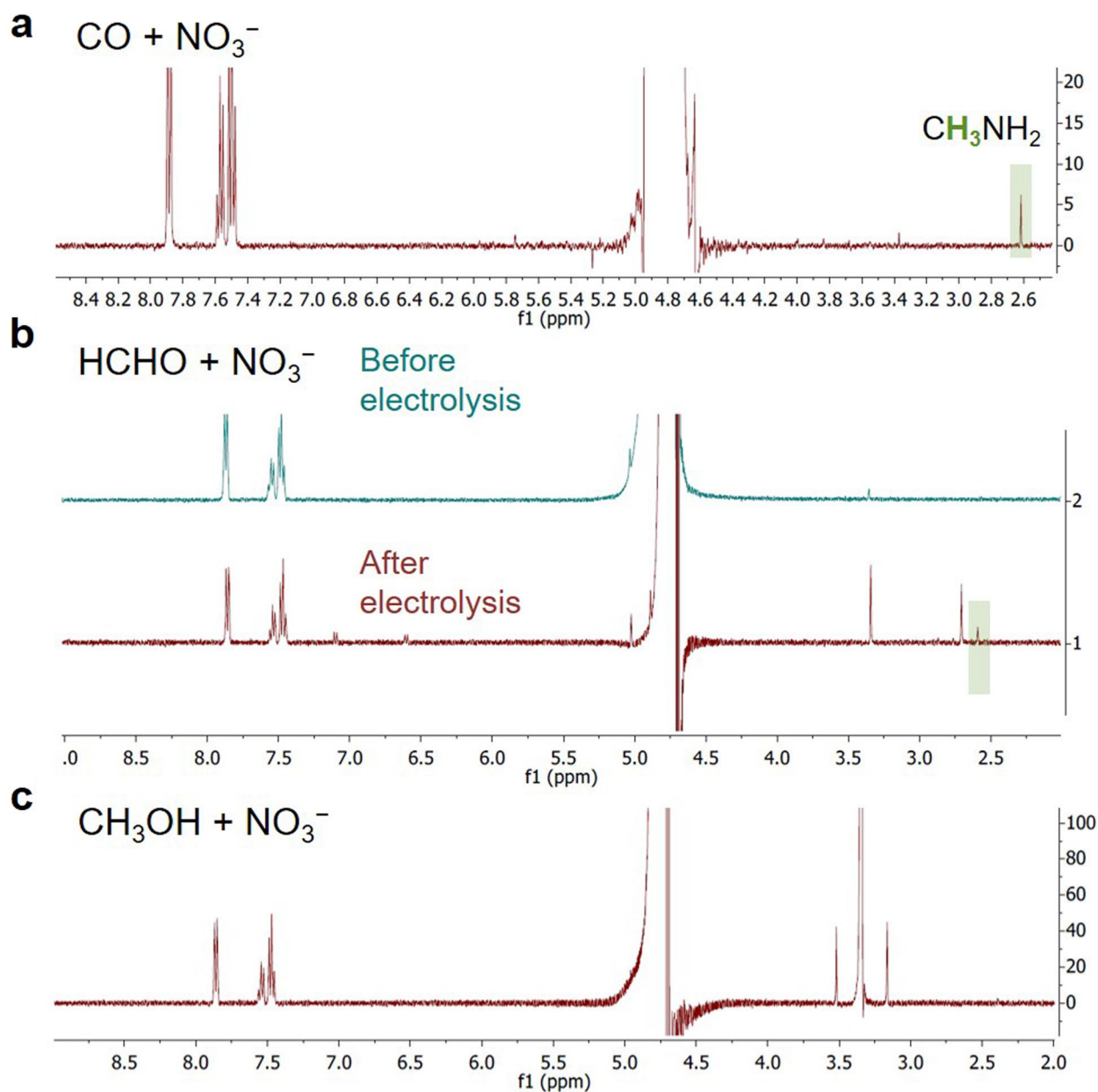


**Extended Data Fig. 5 | Statistics of reaction rate and selectivity.** Potential-dependent **a**,  $j_{\text{methylamine}}$  and **b**,  $FE_{\text{methylamine}}$  values measured from 27 independent co-reduction electrolyses of  $\text{CO}_2$  and  $\text{NO}_3^-$  in 0.1M  $\text{KHCO}_3$  + 0.5M  $\text{KNO}_3$  electrolyte.

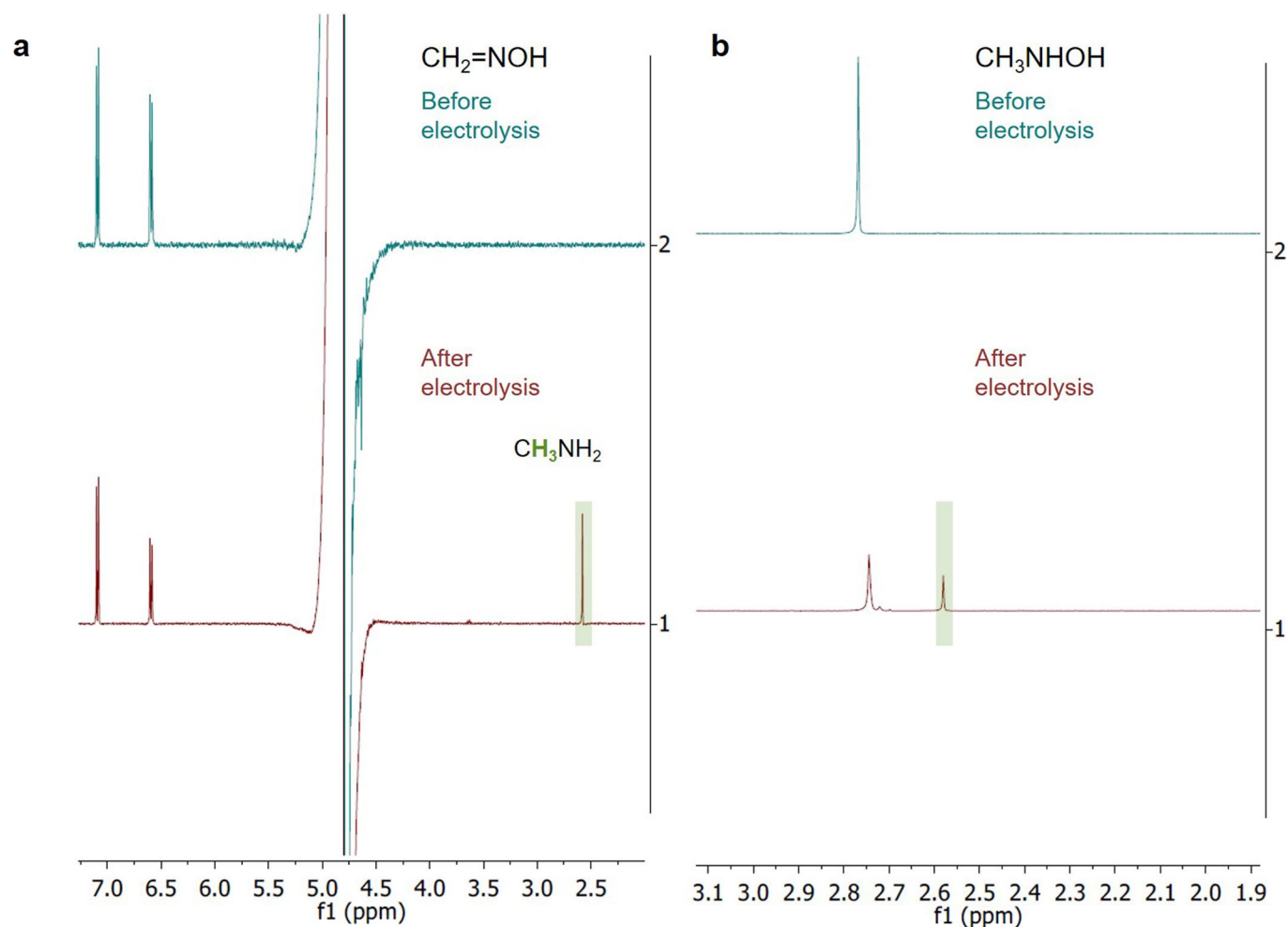


**Extended Data Fig. 6 | Determination of the loading of electrochemically active  $\text{CoPc-NH}_2$  on the electrode.** Integration of the one-electron reduction peak in the cyclic voltammogram to determine the loading of electrochemically active  $\text{CoPc-NH}_2$  molecules. Scan rate:  $10 \text{ mV/s}$ .

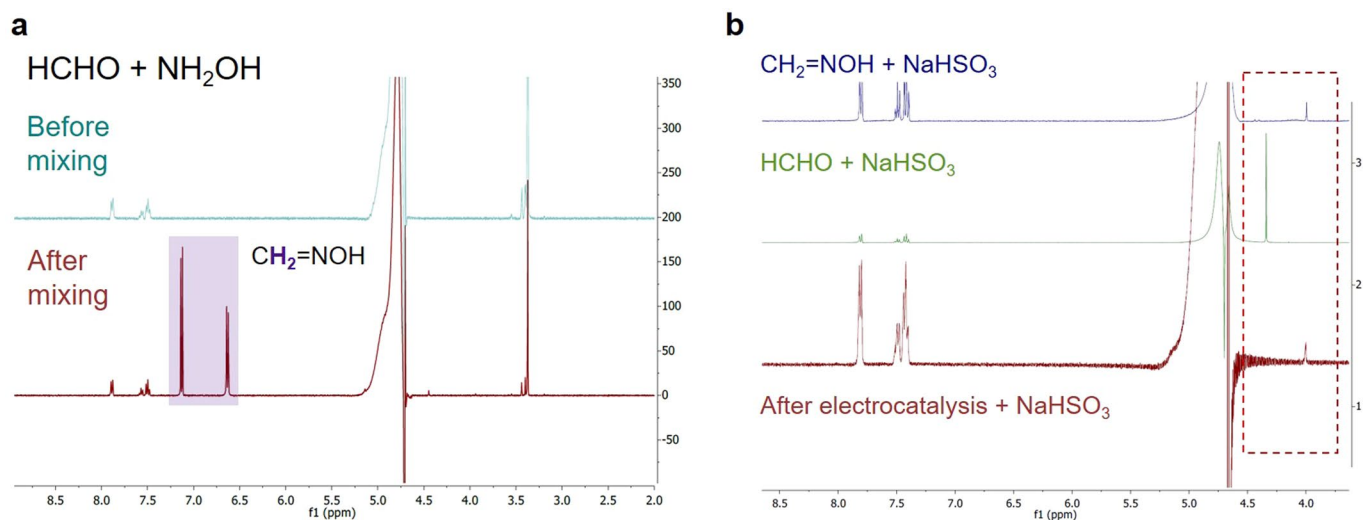




**Extended Data Fig. 8 | Identification of key C intermediates.**  $^1\text{H}$  NMR spectra of catholyte solutions after co-reduction of  $\text{KNO}_3$  with different C sources in 0.1M PBS: **a**, CO, **b**, HCHO and **c**,  $\text{CH}_3\text{OH}$ . The peaks pertaining to methylamine are highlighted in green.



**Extended Data Fig. 9 | Electrochemical reducibility of formaldoxime and N-methylhydroxylamine to methylamine.**  $^1\text{H}$  NMR spectra of catholyte solutions after electroreduction of **a**, formaldoxime and **b**, N-methylhydroxylamine in Ar-saturated 0.1M PBS. The peaks pertaining to methylamine are highlighted in green.



**Extended Data Fig. 10 | Condensation between formaldehyde and hydroxylamine to form formaldoxime. a,** <sup>1</sup>H NMR spectra of 25 mM HCHO dissolved in electrolyte solution before and after adding 50 mM NH<sub>2</sub>OH. Peaks pertaining to formaldoxime are highlighted in purple. **b,** <sup>1</sup>H NMR spectrum of the catholyte solution after co-reduction mixed with 1 M NaHSO<sub>3</sub>. Stacked together are spectra of HCHO and formaldoxime mixed with 1 M NaHSO<sub>3</sub>. Only the reaction product between formaldoxime and NaHSO<sub>3</sub> (~4.00 ppm) but no reaction product between HCHO and NaHSO<sub>3</sub> (~4.39 ppm) can be found.